Mem. S.A.It. Vol. 86, 306

Memorie della

Uncertainties in determining the evolutionary status of unresolved old populations

M. Salaris

Astrophysics Research Institute, Liverpool John Moores University, Twelve Quays House, Birkenhead, CH41 1LD, UK; e-mail: ms@astro.livjm.ac.uk

Abstract. Some major uncertainties in the determination of the evolutionary status of unresolved old stellar populations, using stellar population synthesis models, are presented and discussed. It transpires that the unknown HB morphology of the target populations is a major potential source of error, together with the effect of interacting binaries, usually neglected in stellar population synthesis models. A few techniques aimed at revealing the presence in the target populations of a HB morphology different from the SPSM assumptions are discussed.

Key words. Stars: Population II – Galaxy: globular clusters – galaxies: stellar content

1. Introduction

Investigations of the evolutionary status of unresolved populations rely heavily on the theoretical modelling of the integrated properties of simple stellar populations (SSPs), and eventually of populations with a more complex star formation history. These models are usually named 'stellar population synthesis'models (SPSMs – pioneered in Tinsley 1968)

SPSMs play a major role in investigations about formation and evolution of stellar populations, by means of two opposite/complementary approaches. In what can be named 'inverse'approach, photometric and spectroscopic observations provide empirical integrated spectra and/or colours/magnitudes that are compared to results from SPSMs, to constrain the population star formation histories. The 'direct'approach starts from a theoretical model for the formation of the population under scrutiny, that predicts a specific star formation history. SPSMs convert this theoretical star formation history into expected integrated photometric and spectroscopic properties, that are then compared to their observational counterparts. Mismatches are used as guidelines to refine the theoretical formation model, and the cycle is repeated.

The following sections will briefly highlight some selected issues that one has to face when determining ages and metallicities of unresolved stellar populations using SPSM models, letting aside intrinsic uncertainties due to the choices of stellar evolution models and stellar libraries used in the SPSMs. Attention will be focused here to 'old'populations, whereby 'old'denotes populations with an age above ~1 Gyr, e.g. hosting red giant branch (RGB) stars with an electron degenerate He-core.

2. Low resolution diagnostics

Investigations of unresolved low surface brightness populations, like extragalactic globular clusters, near-field dwarf galaxies and in general distant (high-redshift) galaxies have to make use of diagnostics based on broad band photometry. Figure 1 displays low resolution Spectral Energy Distributions (SEDs) from U to L of three SSPs (6 and 12 Gyr old [Fe/H]=0.06 populations and a 6 Gyr [Fe/H]=−0.25 population) calculated assuming a total mass at birth of $1M_{\odot}$. The SEDs of the two 6 Gyr old SSPs have been shifted (e.g. the total mass rescaled) to have the same I magnitude of the 12 Gyr old one. At fixed [Fe/H], increasing the age causes a shift of the SED towards redder colours, for the integrated magnitudes longward of I become brighter, whilst they become fainter from R to U. On the other hand, keeping the age fixed at 6 Gyr and decreasing [Fe/H] shifts the SED towards bluer colours. This behaviour gives rise to an age-metallicity degeneracy, that is clearly illustrated by comparing the 12 Gyr, [Fe/H]−0.25 SED with the 6 Gyr, [Fe/H]=0.06 one. The U, B, V, R (and I, by construction) magnitudes are essentially identical. Only when moving towards longer wavelengths the differences between the SED of these two populations increase above 0.1 mag.

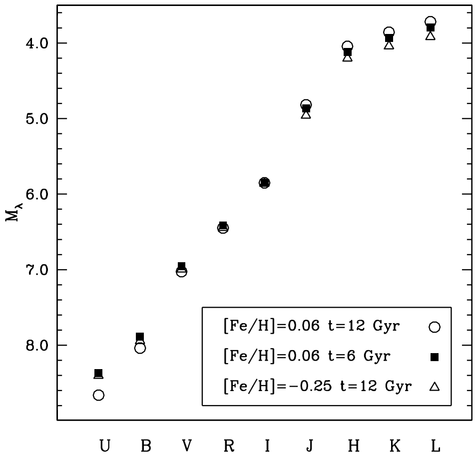

Fig. 1. The age-metallicity degeneracy for low resolution SEDs.

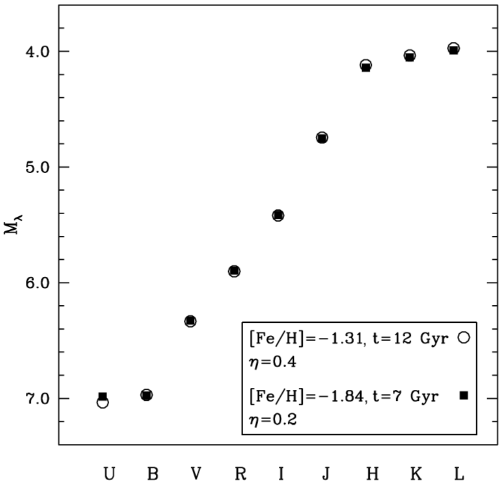

Fig. 2. The age-metallicity-HB morphology degeneracy for low resolution SEDs.

Another important degeneracy for old populations is illustrated by Fig. 2, that displays the SED of a 12 Gyr [Fe/H]=−1.31 population with horizontal branch (HB) colour determined using a Reimers mass loss law along the RGB, with the free parameter η set to 0.4, and a 7 Gyr [Fe/H]=−1.84 η=0.2 SSP. The 7 Gyr SED has been rescaled in mass to have the same I magnitude of the older SSP. After this shift, all magnitudes from B to J are practically identical (differences by less than 0.01 mag), and the differences in H, K and L are equal to just ∼0.02 mag. Only for the U-band the difference increases to 0.05 mag. This age-metallicity-HB colour degeneracy is one of the most serious problems in photometric (and spectroscopic) studies of unresolved old stellar populations, given our current inability to predict the HB morphology of a stellar population of given age and metallicity.

'Classical', distance (and SSP mass) independent techniques make use of colour-colour diagrams that minimize the effect of the age-metallicity degeneracy, i.e. the two colours must show different sensitivities to variations of metallicity and age. Colours restricted to the $BVRI$ bands are severely affected by the degeneracy, that can cause uncertainties by a factor of two on both age and [Fe/H] estimates. Extending the spectral range covered by the observations to the near infrared and/or the U band helps in minimizing the effect of this degeneracy, as was firstly recognized about 30 years ago (Bothun et al. 1984). In a diagram like $(B-V)$-$(V-I)$, sequences of constant age at varying [Fe/H], and sequences of constant [Fe/H] and varying ages overlap almost completely, implying that this diagram is severely affected by the age-metallicity degeneracy. Colour-colour diagrams like $(V-K)$-$(V-I)$ – a tool often used to study extragalactic GCs (see, e.g., Hempel & Kissler-Patig 2004; Hempel et al. 2003) – display constant age and constant [Fe/H] lines that are more orthogonal, i.e. the degeneracy is, to some degree, broken. The 'ideal' colour-colour diagram would display perfectly orthogonal age-metallicity sequences. A recent study of favourable colour combinations to minimize the the age-metallicity degeneracy can be found in Li & Han (2008b). A common feature of these diagrams is the generally poorer age resolution with increasing age. For the VIK diagram this is especially true in the metal poor regime. The best approach in this case is to study statistically the age distribution of large samples of SSPs, for example their cumulative age distributions (see, e.g. Hempel & Kissler-Patig 2004; Salaris & Cassisi 2007). Obviously, the size of the photometric error has a large impact on this type of analyses, e.g. 1σ photometric errors equal to 0.1 mag in the VIK passbands would prevent the detection of bimodal SSP populations with age differences up to ~8Gyr, when the $(V-K)$-$(V-I)$ is employed.

More recently, the use of near- and far-UV filters has been advocated (Kaviraj et al. 2007). At ages above 1 Gyr, for example, the $m(1500)$-$(B-V)$ diagram has been shown to be a promising tool for age and metallicity estimates of SSPs (Yi 2004). A crucial issue related to the use of UV filters is their extreme sensitivity to the presence of hot HB stars. Calibrating the HB morphology-age-metallicity trend in the models, to match the *average* behaviour in Galactic globulars may in principle not produce the correct colours in extragalactic globulars. Another largely unexplored problem, that affects short wavelength filters (starting from U) when hot HB stars are present, is related to the efficiency of atomic diffusion and radiative levitation. Spectroscopic observations of hot HB stars in Galactic globulars (see, e.g. Behr 2003) reveal an increase of the surface abundance of several metals (Fe among them) and a decrease of surface He when $T_{\rm eff}$ increases above ~11500 K. This appears to be caused by the combined effect of atomic diffusion and radiative levitation, that however need to be moderated by additional mixing processes, for theoretical HB models including these processes predict the onset of abundance anomalies at a lower $T_{\rm eff}$ (Quievy et al. 2009). At present no extended and complete – calculated until their transition to the final cooling sequence – grids of hot HB models that reproduce these observations, nor extended grids of appropriate model atmospheres (see, e.g., Leblanc et al. 2010, for explorative studies) are available for population synthesis studies.

A conceptually equivalent method (with the same problems) is obviously the use of the integrated magnitudes themselves. In this case, provided that an independent distance estimates is available, one can also derive stellar masses from the fitting procedure. The work by Anders et al. (2004); de Grijs (2005) introduces fits to the observed broad-band SED from U to H, to determine simultaneously age-metallicity-internal extinction (if any) of SSPs, once distance modulus and foreground extinction are specified. One can in principle disentangle these three free parameters based on the shape of a low resolution SED, and determine the stellar mass of the population by scaling the model magnitudes to the observed level, with a minimum of four passbands – assuming a specific functional form of the internal extinction law and an initial mass function (IMF).

Recent investigations (see, e.g., Li & Han 2008a) have studied the impact of the progeny of binary interactions on the integrated spectra of SSPs. The problem with predicting the effect of binaries on the integrated spectra of SSPs is the large number of free parameters involved, for which there are very few constraints. The main parameters to fix after initial chemical composition and age are chosen, are the IMF of the primary components, the relationship between the mass of the secondary and primary components, the distribution of orbital separations, the distribution of orbital eccentricities, the efficiency of common envelope ejection, the mass loss efficiency for the isolated evolution of the individual component, the efficiency of the tidally enhanced mass loss (compared to the Reimers value) in binary systems. For ages above 1 Gyr binary interactions – due to the appearance of blue stragglers and extreme HB stars – affect the shape of the spectral energy distribution by boosting the flux below a certain threshold wavelenght, that generally decreases with increasing age (at fixed metallicity). Typically, for ages of the order of 10 Gyr, binary interactions modify the shape of the integrated spectrum only below $\lambda \sim 3000$ Å, whilst for ages of the order of 1 Gyr this effect is noticeable already at $\lambda \sim 8000$ Å. The net result is to shift towards the blue of broadband colours that involve these wavelength ranges, as expected.

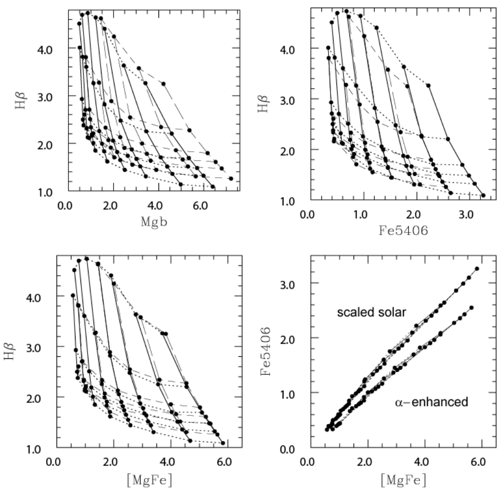

Fig. 3. Several index-index diagrams for scaled solar SSPs (solid and short dashed lines) with [Fe/H] = −1.79, −1.49, −1.27, −0.96, −0.66, −0.35, +0.06, +0.40 and α-enhanced SSPs (long dashed and dotted lines) with [Fe/H] = −1.84, −1.31, −1.01, −0.70, −0.29, +0.05. Metallicity increases from left to right. The ages (increasing from top to bottom) are equal to 1.25, 3, 6, 8, 10, and 14 Gyr.

3. High resolution diagnostics

Integrated spectra of unresolved populations (≈1-10 Å resolution) display absorption features that can be used to constrain stellar ages and chemical compositions. The absorption feature strengths are usually measured by a system of indices – largely unaffected by dust attenuation – that are essentially a measure of their equivalent widths, and then compared to the corresponding theoretical predictions. To date, most of the evolutionary information gathered from the analysis of integrated spectra of old stellar populations has been obtained using the Lick indices in the blue-visual part of the spectrum Worthey et al. (1994).

The Lick system of indices provides powerful index-index diagrams, that break to a large degree the age-metallicity relationship, and can provide in principle solid estimates of age, [Fe/H] and [α/Fe] of a given SSP. Examples of these diagrams are reported in Fig. 3. The top right-hand panel of this figure shows H_β-Fe5406 index grids for a range of metallicities and ages, as detailed in the figure caption, and both scaled solar and α-enhanced ([α/Fe]=0.4) metal mixtures. The two metal mixtures are accounted for consistently in both isochrones and stellar spectra. The top left-hand panel displays a H_β-the Mgb index grid, that demonstrate the sensitivity of the Mgb index to the degree of α-enhancement, because of its dependence on the abundance of Mg. From the indices Fe5406 and Mgb one can calculate the index [MgFe]= $\sqrt{\langle \mathrm{Fe} \rangle \times \mathrm{Mg}b}$, with $\langle Fe \rangle = \frac{1}{2}$(Fe5270+Fe5335), and the bottom left-hand panel of Fig. 3 shows the H_β-[MgFe] diagram. The [MgFe] index appears to be sensitive to the total metallicity Z, without being affected by the degree of α-enhancement. The use of the Fe5406-[MgFe] plane, illustrated in the bottom right-hand panel of Fig. 3, allows the estimate of the degree of α-enhancement. In this plane, the lines of constant age and constant metallicity are almost completely degenerate, however the scaled-solar (upper) and α-enhanced (lower) sequences are clearly separated. Therefore, using a combination of three grids – H_β-Fe5406, H_β-[MgFe], and Fe5406-[MgFe] – it is in principle possible to disentangle age, total metallicity Z, [Fe/H], and the degree of α-enhancement of a SSP.

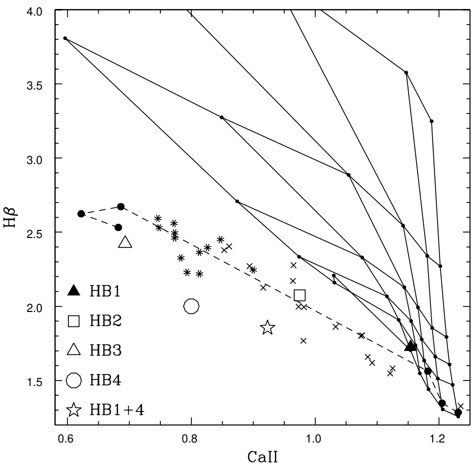

Fig. 4. Index-index diagnostic of the HB morphology (see text for details).

A mismatch between the HB morphology in the target SSP and the adopted SPSMs can cause major errors in the estimate of the population evolutionary properties. Especially when the observed population has a blue HB component – that enhances the strength of the Balmer lines – not represented in the SPSM counterpart, the observed value of the Balmer line indices will be matched with a too young age. This issue has been exhaustively explored in Percival & Salaris (2011). The obvious question to address is whether there are indices that could potentially discriminate between a very old SSP with an extended blue HB and a SSP with an intermediate-old age – i.e., between 3 and 6-8 Gyr; looking at the integrated spectra one immediately realizes that the range to explore is at wavelengths below ~4000-4500 Å. There are at least three different diagnostics proposed in the recent literature (Percival & Salaris 2011; Schiavon et al. 2004). The first one is the ratio between the value of the $H\delta_F$ and H_β indices, that appears to be far more sensitive to HB morphology than to age. In practice, whenever the age obtained from, i.e., the $H\delta_F$-Fe5406 diagram is not the same as the age obtained from the H_β-Fe5406 grid, this could be an indication for the presence of HB stars bluer than in the models. The second potential diagnostic is the Mg II feature around 2800 Å. The value of the associated index displays a strong trend towards lower values as the HBs become more extended towards the blue, at fixed chemical composition. Given that Mgb (another Mg-sensitive index) is negligibly affected by the HB morphology, any discrepancy between the metallicities derived from the Mgb and Mg II indices for a given stellar population could be due to the presence of an extended blue HB component not included in the adopted SPSM calibration. A third potential diagnostic makes use of the $Ca_{II}H + H\epsilon/Ca_{II}K$ index, that for brevity is denoted here as CaII. This index was already identified in Rose (1984) as being sensitive to the presence of hot stars in a composite spectrum. Figure 4 displays a H_β-CaII grid (calculated with Reimers η= 0.2), and indices derived from synthetic HB simulations (for [Fe/H]=−1.3) with extended (in colour) and increasingly blue HB morphologies (from 1 to 4), plus a bimodal HB case (1+4). All the extended HB models lie outside the η= 0.2 grid, except for HB model 1, the red clump case. This means that the H_β-CaII grid could potentially discriminate between an old population with extended blue HB and an intermediate-old age – provided that the correct Ca abundance is accounted for in the theoretical integrated spectra. It is also interesting to consider the sample of Galactic globulars displayed in the diagram as small symbols. The clusters with the bluest HBs fall towards the left-hand side of the H_β-CaII diagram, with lower CaII values. Clusters with HB type >0.8 (predominantly blue HB) are denoted with asterisks and they all fall well outside the reference grid. These same clusters would all appear to have ages around 6-7 Gyr in the H_β-Fe5406 diagram. If their large values of H_β were caused by younger ages rather than blue HBs, these clusters would need to have a higher CaII index for the same H_β strength and the points should be located farther towards the right-hand side of Fig. 4. An important caveat regarding the Ca II index is that it is strongly affected by velocity dispersion, and also requires data with very high signal-to-noise ratio.

One issue still to be comprehensively explored is the effect of radiative levitation, effective in HB stars with T_{eff} above ~12000 K. Some approximate conclusions can however be drawn by assuming that levitation affects just the stellar spectra and can be mimicked by 'standard' spectra with varied individual abundances. Observations of Galactic globulars show that Ca and Mg are basically unaffected by levitation, whereas Fe is always enhanced to solar or supersolar values. It is therefore natural to speculate whether an enhanced Fe content for hot HB stars could affect the behaviour of iron-sensitive indices. In absence of detailed calculations, one can just notice that the Fe5406 index seems weakly sensitive to blue HB stars, especially when T_{eff} increases above ~10000 K. This leads to the tentative conclusion that most probably iron-sensitive indices are only very mildly affected by levitation.

As for the effect of binary interactions, because of the presence of binary-produced Blue Stragglers and hot HB stars, the Balmer line indices increase, mimicking spuriously young ages when binary interactions are not accounted for in SPSMs. Also, the effect on the Fe and [MgFe] indices is to underestimate [Fe/H] and Z.

4. Conclusions

A very short summary of some major uncertainties in the determination of the evolutionary status of unresolved old stellar populations has been presented. For both low- and high-resolution diagnostics, the unknown HB morphology of the target population is a major uncertainty, together with the potential effect of interacting binaries, usually neglected in SPSMs. A few promising techniques, to reveal the presence in the target populations of a HB morphology different from the SPSM assumptions, have been put forward by different authors. A wide application to observed systems is still lacking.

References

Anders, P., et al. 2004, MNRAS, 347, 196
Behr, B. B. 2003, ApJS, 149, 67
Bothun, G. D., et al. 1984, AJ, 89, 1300
de Grijs, R., Anders, P., Lamers, H. J. G. L. M., et al. 2005, MNRAS, 359, 874
Hempel, M., & Kissler-Patig, M. 2004, A&A, 419, 863
Hempel, M., et al. 2003, A&A, 405, 487
Kaviraj, S., et al. 2007, MNRAS, 381, L74
Leblanc, F., Hui-Bon-Hoa, A., Khalack, V. R. 2010, MNRAS, 409, 1606
Li, Z., & Han, Z. 2008a, MNRAS, 685, 225
Li, Z., & Han, Z. 2008b, MNRAS, 385, 1270
Percival, S. M., & Salaris, M. 2011, MNRAS, 412, 2445
Quievy, D., et al. 2009, A&A, 500, 1163
Rose, J. A. 1984, AJ, 89, 1238
Salaris, M., & Cassisi, S. 2007, A&A, 461, 493
Schiavon, R. P., Rose, J. A., Courteau, S., & MacArthur, L. A. 2004, ApJ, 608, L33
Tinsley, B. M. 1968, ApJ, 151, 547
Worthey, G., Faber, S. M., Gonzalez, & J. J., Burstein, D. 1994, ApJS, 94, 687
Yi, S. K. 2004, ApJ, 582, 202